The Wind Structure in Planetary Boundary Layer

Zhao Ming (赵鸣) *Xu Yinzi* (徐银梓) and *Wu Rongsheng* (伍荣生)
Department of Atmospheric Sciences, Nanjing University, Nanjing
Received February 2, 1988

ABSTRACT

The investigations on the dynamics of the PBL have been developed in recent years. Some authors emphasized macro-dynamics and others emphasized micro-structure of the PBL. In this paper, we study and review some main characteristics of the wind field in the PBL from the view point connecting the macro-dynamics and micro-stucture of the PBL, thus providing the physical basis for the further research of the dynamics and the parameterization of the PBL.

I. INTRODUCTION

Different methods are used in the studies of the PBL dynamics. In the surface layer, some authors emphasized to research the characteristics of the micro-structure on account of the plentiful observation data. As to the Ekman layer or whole PBL, less achievements have been made than that for the surface layer because the data are not enough. The researches for the whole PBL are mainly about the macro-dynamics and the parameterization of the PBL, these studies are promoted by researches of the numerical weather prediction and the numerical experiment of the general circulation.

Connecting these two kinds of researches is a significant work, which can build the dynamics of the PBL on the basis of the micro-structure and support the research of micro-structure of the PBL on the background of large-scale dynamics. This work may not only understand the dynamics characteristics of the PBL in detail, but also provide the physical basis for the parameterization research and the numerical modelling of the circulation.

In this paper, we shall describe and review our recent work based on the previous viewpoint. For the micro-structure of the PBL, we mainly consider the accurate treatment for the eddy coefficient and the effect of thermal stratification which are the main factors affecting the distribution of wind and temperature in the PBL.

II. THE BOUNDARY LAYER FLOW WITH THE EQUILIBRIUM OF FOUR FORCES

The classical Ekman theory was based on the equilibrium of three forces, pressure gradient force, Coriolis force and turbulent friction force, from which the wind spiral in the PBL was derived. It was found from the further investigation on the meso-scale system that the inertial force can not be neglected in some systems. Wu and Blumen (1982) applied geostrophic momentum approximation to study the characteristics of the wind distribution in the PBL under the assumption of the equilibrium between the four forces including the inertial force. Because the advected parts of the advection terms in the inertial force were substituted by geostrophic wind and the advecting parts still contained the ageostrophic components, hence, the flow across isobar could cause frontogenesis or the development of system,

this was the superiority of the geostrophic momentum approximation, at the same time, the geostrophic momentum approximation might simplify the problem in the condition of given pressure field or the geostrophic wind field.

With the geostrophic momentum approximation, the nondimensionalized motion equation can be written as:

$$Ro(\frac{\partial}{\partial t} + \vec{v} \cdot \nabla)\vec{v}_g - \vec{k} \wedge (\vec{v} - \vec{v}_g) = \frac{1}{2}\frac{\partial^2 \vec{v}}{\partial z^2}, \tag{1}$$

$$\eta = \frac{z}{(2E)^{1/2}}, \tag{2}$$

where Ro, E are the Rossby number and Ekman number respectively.

The boundary conditions are:

$$u = v = w = 0, \quad \text{where} \quad \eta = 0; \tag{3}$$
$$u, v, w \text{ are limited, where } \eta \to \infty.$$

with condition (3) and given pressure field, not considering the temperature difference in the PBL, we may obtain the solution of Eq.(1) as:

$$u = u_T(1 - e^{-\beta}\cos\beta) - c_1 D^{-2} e^{-\beta}\sin\beta,$$
$$v = v_T(1 - e^{-\beta}\cos\beta) - c_2 D^{-2} e^{-\beta}\sin\beta, \tag{4}$$

where $\beta = D\eta$ and

$$D^4 = 1 + Ro\zeta_g + Ro^2\left(\frac{\partial u_g}{\partial x}\frac{\partial v_g}{\partial y} - \frac{\partial v_g}{\partial x}\frac{\partial u_g}{\partial y}\right). \tag{5}$$

ζ_g is geostrophic vorticitg, u_T, v_T are the wind speeds at the top of the PBL:

$$u_T = -\frac{Ro(v_g + Ro\frac{\partial u_g}{\partial t})\frac{\partial v_g}{\partial y} - (u_g - Ro\frac{\partial v_g}{\partial t})(1 - Ro\frac{\partial u_g}{\partial y})}{1 + Ro(\frac{\partial v_g}{\partial x} - \frac{\partial u_g}{\partial y}) + Ro^2(\frac{\partial u_g}{\partial x}\frac{\partial v_g}{\partial y} - \frac{\partial v_g}{\partial x}\frac{\partial u_g}{\partial y})}, \tag{6a}$$

$$v_T = \frac{Ro(u_g - Ro\frac{\partial v_g}{\partial t})\frac{\partial u_g}{\partial x} + (v_g + Ro\frac{\partial u_g}{\partial t})(1 + Ro\frac{\partial v_g}{\partial x})}{1 + Ro(\frac{\partial v_g}{\partial x} - \frac{\partial u_g}{\partial y}) + Ro^2(\frac{\partial u_g}{\partial x}\frac{\partial v_g}{\partial y} - \frac{\partial v_g}{\partial x}\frac{\partial u_g}{\partial y})}, \tag{6b}$$

when $Ro \to 0$, $D \to 1$, Eq.(4) becomes the classical Ekman spiral. When $Ro \neq 0$, the wind structure will change because of the inhomogeneity of the geostrophic wind field. In order to show this phenomenon, we assume that the pressure field is (r is nondimensional radius, φ the nondimensional geopotential deviation):

$$\varphi = \pm(1 - \frac{\alpha}{2}r^2)e^{-\frac{\alpha}{2}r^2}, \tag{7}$$

where α is a constant. The pressure field (7) is an axisymmetric high or low, the plus sign is for the high and the minus is for the low. The geostrophic wind speed is $\partial\varphi / \partial r$. The wind distribution at $r = 1$ in case of $\alpha = 1/2$ is shown in Fig.1. It can be seen that when $Ro = 0$, the curve is just the classical Ekman spiral which does not include the effect of the geostrophic momentum. The distributions are different when the geostrophic momentum is taken into account. The wind approaches its value at the top of the PBL faster in cyclone than

that for the Ekman spiral and vice verse in anticyclone. This reflects the effects of the inertial force and this conclusion improves the Ekman theory.

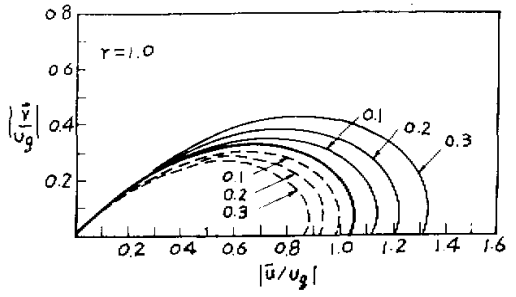

Fig.1. The traces of the velocity vector end of the PBL wind at $r = 1$ in case of $\alpha = 0.5$, the figures on the curves are the Ro number, the solid line represents anticyclone, dashed line represents cyclone, the X axis is along the isobar.

III. THE THREE SECTIONS K MODEL AND N-SECTIONS K MODEL

The above-mentioned PBL model with the geostrophic momentum approximation shows the important role played by the inertial force and simplifies the calculation for nonlinear terms, hence, it is an improvement to the PBL model. But the treatment of K = const is not rigorous on account of this treatment, the wind speed near the surface is too small and the angle α between the wind near the surface and the geostrophic wind is too great (45°, and constant) to be compared with the realistic wind. The reason is that near the surface, the magnitude of constant K which represents the mean K throughout the whole PBL is much larger than the realistic one there, which results in too small a dv/dz near the surface because the stress is constant in the surface layer. Consequently, the wind speed near the surface will be too low, the constant $\alpha = 45°$ is also a result of K = const. We apply different treatments to overcome this shortcoming, one of them is to assign different values for K in different height ranges. Xu et al. (1988) devided the PBL into three sections, different values of K were taken in these three sections to express the realistic K distribution approximately.

The first section is the surface layer, the well-known linear distribution for K is taken, which expresses the K distribution in the neutral surface layer precisely; the different constant values are taken for K in the second and third sections, i.e.,

$$K = \begin{cases} K_1 z & (z_0 \leqslant z < h_1) \\ K_2 = K_1 h_1 & (h_1 \leqslant z < h_2) \\ K_3 & (K_3 < K_2)\ (h_2 \leqslant z) \end{cases}, \tag{8}$$

where the magnitude of K corresponds to the K value at 1m, z_0 is the roughness. According to (8), the logarithmic distribution for the wind speed in the surface layer is thus obtained which is in agreement with the general law. We then try to find the solutions under the assumption of the equilibrium between the four forces in the second and third sections, some concerned constants are determined from the continuity conditions for the wind speed and the stress at the boundaries between different sections. The derived wind distributions in the three sections are:

$$u_1 = 2h_1 Re\{E_1\}\ln\frac{z}{z_0}, \quad v_1 = 2h_1 Re\{E_1 A\}\ln\frac{z}{z_0},$$

$$u_2 = u_T + 2Re\left\{(D_1 + c_1c_2D_2)e^{r_2z} + c_2D_2e^{-r_2z}\right\},$$

$$v_2 = v_T + 2Re\left\{\left[(D_1 + c_1c_2D_2)e^{r_2z} + c_2D_2e^{-r_2z}\right]A\right\}, \tag{9}$$

$$u_3 = u_T + 2Re\left\{D_2e^{-r_3z}\right\}, \quad v_3 = v_T + 2Re\left\{D_2e^{-r_3z}A\right\},$$

where u_T, v_T are expressed by (6). The complex constants r_2, r_3, E_1, A, C_1, C_2, D_1 and D_2 are determined from the geostrophic wind and its first order derivatives. Applying the pressure field (7), taking $f = 10^{-4}s^{-1}$, the length scale 10^6 m. velocity scale 30 m/s (corresponds to $Ro = 0.3$), we obtain the traces of the wind vector end at $r = 1$ as in Fig.2. It is shown that the speeds near the surface are much greater than that obtained from constant K (i.e. the results in Wu and Blumen 1982), at the same time, the angle between the wind near the surface and the geostrophic wind is smaller than the latter, all of these are more in agreement with reality. This is because K has been improved. Meanwhile, the wind differences in different pressure fields deduced from the geostrophic momentum approximation are still retained which characteristics are the same as in Fig.1.

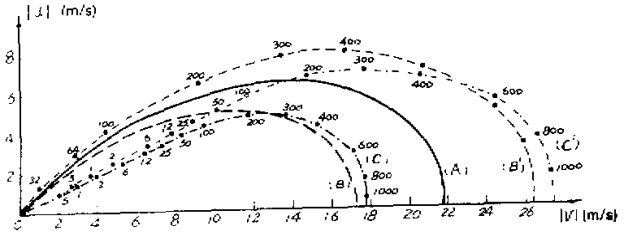

Fig.2 The wind distribution in the PBL with the geostrophic momentum approximation and three sections **K**, the X axis points forward to outside along the radius $z_0 = 0.1$ m, $h_1 = 50$ m, $h_2 = 250$ m. (A) is the classical EK man solution; (B), (B') are the solutions in cyclone and anticyclone respectively with the geostrophic momentum approximation and constant **K**; (C), (C') are the solutions in cyclone and anticyclone respectively with the geostrophic momentum approximation and three sections **K**.

From mixing length theory, we have:

$$K_1 = kv_*, \qquad v_* = |K\frac{\partial v_1}{\partial z}|, \tag{10}$$

where k is Karman constant, and 0.4 is taken for its value, v_* the friction velocity. Substituting the derived wind distribution into (10), we have an implicit equation to determine K_1 and which can easily be found by iteration method. It is found that the derived K_1 depends on the geostrophic wind, therefore, K_1 is a function of x, y, z, t, this treatment is an improvement to the classical solution which can not determine K objectively.

The above-mentioned three sections K model is suitable for the barotropic and neutral conditions. Introducing thermal wind and Businger's universal function, the analytic solutions for baroclinic and non-neutral conditions have already been obtained.

Because the K value in the third section is difficult to be determined objectively and to divide the PBL into three sections is too rough after all, Xu (1989a) extended the three sections K model to N–sections K model (N is an arbitrary positive integer). The first section is identical to the three sections K model, the Ekman layers are devided into N–1 sections.defferent constant K values are taken for those N–1 sections, these constants K are determined from O'Brien formula (O'Brien, 1970) which is an appropriate cubic polynomial expressing the realistic K distribution in the PBL and be widely used in the numerical modelling for the PBL. The method for solving the wind distribution in the N–sections K model is similar to the three sections K model.

We may also utilize the small parameter expansion method which is usually applied in the nonlinear technique to study the motion with the equilibrium between the four forces except the geostrophic momentum approximation. Wu (1984) derived the solution for the problem of the equilibrium between the four forces by use of the constant K, after that, Xu (1989b) extended that work to the baroclinic and non–neutral conditions and three sections K model. The wind distributions calculated from these works also reflects the effects of the temporal and spatial variations of the pressure field and the results are reasonable. These works both have theoretical and applied significance.

IV. THE WIND FIELD IN THE PBL WITH NON–LINEAR EDDY COEFFICIENT

In order to precisely simulate the wind distribution in the PBL, the eddy coefficient K derived from the turbulence theory is usually applied in modern PBL dynamics, i.e., K is assumed to be connected with the vertical distribution of wind speed and the mixing length. K is treated as an unknown function to be solved from motion equations with wind field simultaneously. This treatment not only can obtain the realistic wind distribution, but also the realistic objective K distribution and other boundary layer parameters. The characteristics of the PBL are shown more perfectly. The published works utilizing the nonlinear K are usually based on the equilibrium between three forces. Zhao (1988a) applied the above–mentioned K in the equation of the equilibuium between four forces with the geostrophic momentum approximation, i.e., the following K was chosen (Bhumralkar, 1975)

$$K = l^2 + \left[\left(\frac{\partial u}{\partial z}\right)^2 + \left(\frac{\partial v}{\partial z}\right)^2 \right]^{1/2}, \tag{11}$$

where l was the mixing length. By use of this K expression, the dimensional PBL equation with the geostrophic momentum approximation can be solved:

$$\frac{\partial \vec{v}_g}{\partial t} + (\vec{v} \cdot \nabla)\vec{v}_g = \vec{k} \wedge (\vec{v} - \vec{v}_g) + \frac{\partial}{\partial z}\left(K \frac{\partial \vec{v}}{\partial z}\right) \tag{12}$$

and the wind distribution in the neutral, barotropic PBL is thus obtained under the assumption of the equilibrium of four forces and the nonlinear K. The upper boundary condition for Eq. (12) is the dimensional form corresponding to Eq. (6):

$$u_T = \frac{(u_g - \frac{1}{f}\frac{\partial v_g}{\partial t})(1 - \frac{1}{f}\frac{\partial u_g}{\partial y}) - (v_g + \frac{1}{f}\frac{\partial u_g}{\partial t})\frac{1}{f}\frac{\partial v_g}{\partial y}}{1 + \frac{1}{f}(\frac{\partial v_g}{\partial x} - \frac{\partial u_g}{\partial y}) + \frac{1}{f^2}(\frac{\partial u_g}{\partial x}\frac{\partial v_g}{\partial y} - \frac{\partial v_g}{\partial x}\frac{\partial u_g}{\partial y})}, \tag{13a}$$

$$v_T = \frac{(v_g + \frac{1}{f}\frac{\partial u_g}{\partial t})(1 + \frac{1}{f}\frac{\partial v_g}{\partial x}) + (u_g - \frac{1}{f}\frac{\partial v_g}{\partial t})\frac{1}{f}\frac{\partial u_g}{\partial x}}{1 + \frac{1}{f}(\frac{\partial v_g}{\partial x} - \frac{\partial u_g}{\partial y}) + \frac{1}{f^2}(\frac{\partial u_g}{\partial x}\frac{\partial v_g}{\partial y} - \frac{\partial v_g}{\partial x}\frac{\partial u_g}{\partial y})}. \tag{13b}$$

The lower boundary condition is taken as the non-slip condition. The following l is taken according to modern PBL model:

$$l = \frac{0.4(z + z_0)}{1 + \frac{0.4(z + z_0)}{\lambda}}, \tag{14}$$

$$\lambda = 0.0063\frac{u_*}{f}. \tag{15}$$

u_* is the friction velocity. Because z_0 is contained in the l expression, so that the solution of Eq.(12) reflects the effects of z_0. Figs.3 and 4 depict the wind distributions in the cyclone and anticyclone (7) at $r=1$ when $L=10^6$ m, $U=30$ m/s, $f=10^{-4}$ s^{-1}(corresponding geostrophic wind speed is 20.44 m/s), it is shown that the wind speed near the surface and the angle between the surface wind and the geostrophic wind both approach the realistic data. The derived geostrophic drag coefficient $C_g = u_* / G$ (G is the geostrophic wind speed) is 0.028 in the cyclone and 0.036 in the anticyclone. These values are in agreement with the observational data $C_g \approx 0.03$ in the case of the boundary layer Rossby number $Ro = G/fz_0 = 2\times 10^7$. Because $u_T = 0$ in this example, v_T is larger in the anticyclone than that in the cyclone, hence the u_* is larger in the anticycolne.

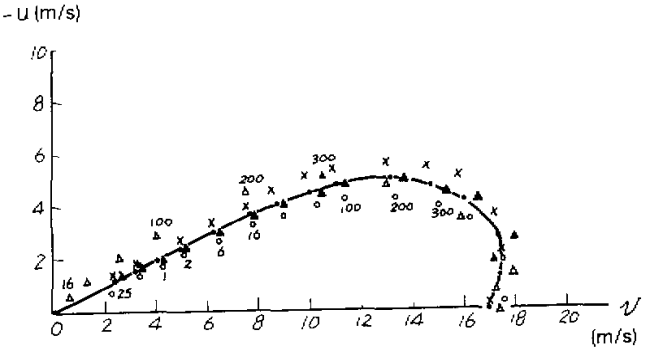

Fig.3. The numerical solution for the trace of the wind vector end in the cyclone (represented by.) and the results of Wu and Blumen (1982). $z_0 = 1$ cm.

In order to coincide the realistic atmospheric condition further, Zhao (1988b) extended Eq.(12) to the baroclinic and non-neutral atmosphere, the effects of thermal stratification were expressed by its effects on the K (Bhumralkar, 1975)

$$K = l^2\left[\left(\frac{\partial u}{\partial z}\right)^2 + \left(\frac{\partial v}{\partial z}\right)^2 - \frac{g}{\theta}\frac{\partial \theta}{\partial z}\right]^{1/2}, \tag{16}$$

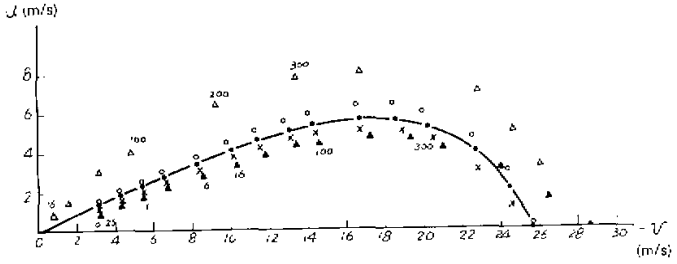

Fig.4. The numerical solution for the trace of the wind vector end in the anticyclone, the legend is identical to Fig.3.

the potential temperature θ in (16) might be found by solving the thermodynamics equation in the PBL simultaneously

$$\frac{d\theta}{dt} = \frac{\partial}{\partial z}(K\frac{\partial \theta}{\partial z}) + S. \tag{17}$$

S was radiation term. We can get the solution in the baroclinic condition if $\vec{V}_g$ in Eq.(12) is taken a known function of height. The numerical solutions for different stratifications and baroclinities are in agreement with the characteristics of the wind in the baroclinic and non-neutral PBL. We try to combine this model with large-scale model and attempt to predict the PBL wind, the primary results show that this is usable.

In modern PBL dynamics, when the K in (11) is used to solve the PBL equation, the surface usually is land, the z_0 is treated as a constant, even on water surface, the z_0 is usually assumed as a small constant. Zhao (1987a) studied the structure of the wind field on water surface with varying roughness, the following z_0 was taken (Garratt, 1977):

$$z_0 = \alpha\frac{u_*^2}{g}, \tag{18}$$

where α was an experimental constant, by use of Eq.(11), the steady, neutral PBL equation with the equilibrium between three forces was solved numerically, the lower boundary was set a very low height near the mean water level, the condition at the lower boundary was:

$$\frac{\partial v}{\partial z} = \frac{u_*}{K(z + z_0)}, \tag{19}$$

$V = \sqrt{u^2 + v^2}$. The derived wind field was in agreement with some characteristics of the wind over sea surface. Because the varying roughtness is used, so that the dependence of z_0 on the wind speed can be reflected in the derived wind field. When the wind speed is low, the flow can be treated as smooth, in the case, instead of (18),

$$z_0 = \nu / 9u_* . \tag{20}$$

where ν is molecular viscosity coefficient. Numerical modelling proves that the geostrophic wind speed $G \gtrsim 5$ m/s may be taken as the criterion distinguish the rough and smooth flows. Therefore, the PBL wind can be solved as long as the geostrophic wind and latitude are known, the work has its practical significance. Fig.5 depicts the wind speed V and wind di-

rection (expressed in terms of the angle between the geostrophic wind and the wind at a certain height) at $\varphi = 40^\circ$ in the cases of different geostrophic wind speeds.

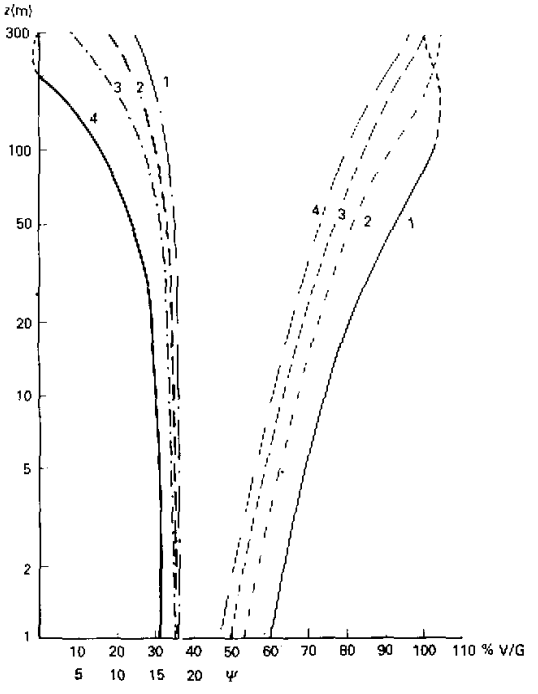

Fig.5. The PBL wind distribution at $\varphi = 40^\circ$, $V = \sqrt{u^2 + v^2}$, ψ is the angle between the geostrophic wind and the wind at a certain height, V/G is in the right, ψ in the left, dotted line represents the parts $V/G > 1$ and $\psi < 0$. 1. $G = 5$ m/s; 2. $G = 10$ m/s; 3. $G = 15$ m/s; 4. $G = 20$ m/s.

Zhao (1988c) studied the PBL over sea in the non-neutral condition, and obtained the wind field in the PBL when the geostrophic wind and the air-sea temperature difference were known, the K satisfied the following relation:

$$K = \left(k \left| \frac{\partial \vec{V}}{\partial z} \right|^2 + \frac{\nu g H}{C_D \rho T} \right)^{1/3} l^{4/3}, \tag{21}$$

where ν is a constant, H the eddy heat flux which can be incorporated into the closed equation set through the formuta of the surface layer in terms of the air-sea temperature difference. The results of the model are also in agreement with the characteristics of the PBL wind field over sea surface. The equations and the boundary conditions are identical to the neutral conditions.

In the Zhao (1988b)'s work, the above-mentioned varying lower boundary condition was applied in the equilibrium equation between the four forces with the geostrophic momentum approximation, and might be used to diagnose the wind field in the PBL over sea.

So far, the study of the PBL dynamics is mainly restricted in the case of straight isobars when K in Eq.(11) is taken, Zhao (1983,1987b) solved the perfect PBL equations including the advection terms to calculate the wind field in the circular vortexes, the wind distribution in the PBL which was commonly determined by the advection and the curvature of the isobars was

obtained. The main characteristics of the wind field in the cyclone and anticyclone were in agreement with the results of the geostrophic momentum approximation, but more detailed resülls were evaluated. These works are profitable for the diagnosis and prediction of the PBL wind in the circular pressure systems.

V. THE VERTICAL VELOCITY AT THE TOP OF PBL IN DIFFERENT MODELS

The vertical velocity at the top of the PBL is a channel of the interaction between the PBL and free atmosphere, its research has its important significance to understand the interaction between the upper and lower atmosphere.

When we apply the geostrophic momentum approximation and the nonlinear technique to study the flow under the equilibrirm among the four forces, the vertical velocity at the top of the PBL is derived at the same time. Wu and Blumen (1982) approximately obtained the nondimensional vertical velocity at the top of the PBL by use of the PBL wind in (4) and the continuity equation as the following equation when the expansion was truncated up to the first order of Ro:

$$w_T \approx \frac{1}{2}(\zeta_g + \frac{1}{4} Ro \frac{\partial \zeta_g}{\partial t} - \frac{3}{4} \mathrm{Ro} \vec{k} \nabla \times \zeta_g \vec{v}_g). \tag{22}$$

If $Ro=0$, i.e., the geostrophic momentum approximation is not included, $w_T \approx \frac{1}{2}\zeta_g$ which is the Charney–Eliassen's classical result. It is seen from Eq.(22), under the assumption of the geostrophic momentum approximation, the vertical velocity at the top of the PBL not only depends on the pressure field, but also the temporal and spatial variations of the geostrophic vorticity. This result should be more reasonable than the classical one because more physical conditions are included.

The vertical velocity at the top of the PBL in the pressure field (7) is shown in Fig.6. We can see from Fig.6. that there exists rise movement in the cyclone and sink in the anticyclone, the intensities are greatest in the centers. When $Ro=0$, the magnitudes of the vertical velocity are identical for the cyclone and anticyclone with the same intensities. But for $Ro\neq 0$, i.e., the geostrophic momentum approximation is included, the vertical velocities in the cyclone are weaker than that for $Ro=0$, and vice versa for the anticyclone. This phenomenon is caused by centrifugal force, the role of the centrifugal force enhances the divergence in the anticyclone and offsets the convergence in the cyclone, and results in the change of the vertical velocity at the top of the PBL.

Fig.7 shows the vertical velocities at the top of PBL derived from Xu et al. (1988)'s three sactions K model with the geostrophic momentum approximation in the pressure field (7) when $f=10^{-4}$ s^{-1}, the length scale $L=10^6$ m and $Ro=0.3$. It is shown that the characteristics of the difference between the cyclone and anticyclone are similar by use of the three sections K model and the constant K model, both include the efffects of the inertial force. The difference between these two models is shown in the values in these two models, for the three sections K model, the geostrophic wind speed approaches zero and hence, K approahes zero at the center, this results in very small vertical velocity; for the constant K model, the effect of varying K does not appear.

Zhao (1987c) suggested a parameterized expression for the vertical velocity at top of the PBL on the basis of a PBL model in which a kind of realistic K was chosen. According to modern PBL numerical model (Nieuwstadt, 1983), the nondimensional K may be expressed by a cubic polynomial:

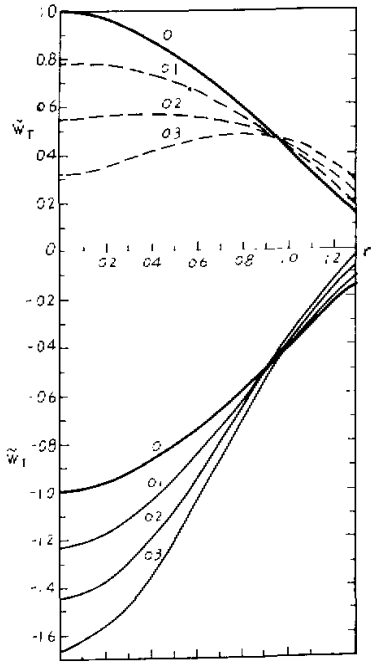

Fig.6 The vertical velocities at the top of the PBL at different radii, the upper part is for the cyclone, the lower part for the anticyclone, the figures on the curves are Ro numbers. $W_T = 1$ corresponds to $w \approx 10^{-2}$ m/s when $E = 10^{-4}$.

$$K = C\eta(1-\eta)^2, \tag{23}$$

where c is an experimatal constant, $\eta = z/h$, h is the PBL height. The K in (23) is nondimensionalized by u_*, h, u_* depends on the geostrophic wind speed, therefore, K is a function of the geostrophic wind, the wind field in the PBL may be obtained by solving one-dimensional PBL equation with the K in (23):

$$W = W_g\left[1 - \frac{(1-\eta)^{\alpha-1}F(\alpha-1,\alpha+1.2\alpha,1-\eta)}{(1-\eta_0)^{\alpha-1}F(\alpha-1,\alpha+1,2\alpha,1-\eta_0)}\right], \tag{24}$$

$W = u + iv$, $W_g = u_g + iv_g$ is complex geostrophic wind speed, $\alpha = \frac{1}{2} + \frac{1}{2}\sqrt{1+4iQ}$, $Q = fh/cu_*$, F is hypergeometric series, η_0 the nondimensional roughness. By use of the continuity equation and the method which is similar to that classial one used by Charney-Eliassen, the dimensional vertical velocity at the top of the PBL is derived:

$$W_T = \zeta_g \frac{0.007G}{f\ln(h/z_0)}. \tag{25}$$

Eq.(25) shows that not only ζ_g, but also the geostrophic wind speed G affects the w_I, this is because G influences the wind speed in the PBL, thus also influences K and $|w_I|$. Eq.(25) also shows the effect of the roughness, the greater the z_0, the greater the $|w_I|$ will be, this is also reasonable. Because more factors are included in Eq. (25), obviously it improves the classical C–E formula.

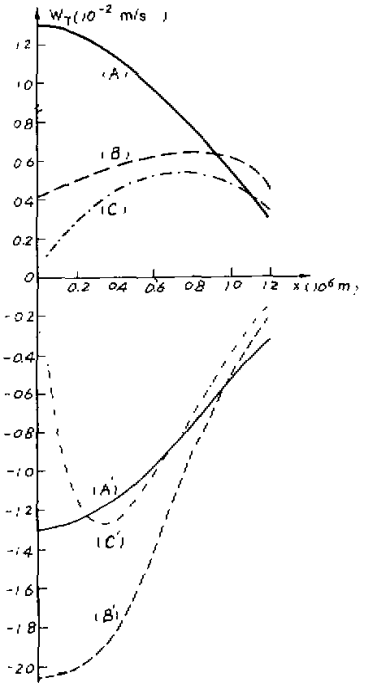

Fig.7. The dimensional vertical velocities at the top of the PBL for three solutions. 1. classical C–E solution (A) cyclone (A') anticyclone; 2.the geostrophic momentum approximation with constant K; (B) cyclone (B') anticyclone; 3. the geostrophic momentum approximation with three sections of K; (C) cyclone (C') anticyclone

VI. CONCLUDING REMARKS

The investigation of the wind field in the PBL is profitable not only for the prediction of the PBL, but also for the parameterization of the PBL in the large–scale models and other dynamics problems. The Characteristic of our work is the combination of the large–scale background field and the modern PBL model, the derived PBL wind field not only precisely reflects the characteristics of the realistic PBL, but also reflects the effect of the large scale background field, therefore, the results may embody the objective reality appropriately. our work not only can be used in the practical prediction, but also can provide the basis for the parameterization of the PBL and other atmospheric dynamics problems.

This paper introduces some works of ours in recent years, some problems should be studied further, especially, the dynamics problems concerned with the wind field in the PBL.

REFERENCES

Bhumralkar,C.M.(1975). A survey of parametrization technique for the PBL in atmospheric circulation models, R-1653 ARPA. ORDER No. 189-1.

Garratt, J.G. (1977). Suggested revision to certain boundary layer parametrization schemes used in atmospheric circulation models, *Mon. Wea. Rev.*, **105:** 915-929.

Nieuwstadt, F.T.M. (1983). On the solution of the stationary baroclinic Ekman layer equations with a finite boundary layer height, *Boundary layer Meteor.*, **26:** 377-390.

O'Brien, J. (1970). A note on the vertical structure of the eddy exchange coefficient in the PBL, *J.Atmos.Sci.*, **27:** 1213-1215.

Wu, R. (1984). Dynamics of non-linear Ekman boundary layer, *Acta. Meteor. Sinica*, **42:** 269-278 (in Chinese with English abstract).

Wu, R. and Blumen, W. (1982). An analysis of Ekman boundary layer dynamics incorporating the geostrophic momentum approximation, *J. Atmos. Sci.*, **39:** 1174-1182

Xu, Yinzi (1989a). The applications of the geostrophic momentum approximation and O'Brien formula, to be published in *Sci. Atmos. Sinica*.

Xu, Yinzi (1989b). The wind in the baroclinic boundary layer with three sublayers incorporating the weak non-linear effect, to be published in *Adv. Atmos. Sci.*

Xu, Yinzi and Zhao, M. (1988). The motions in the boundary layer under the geostrophic momentum approximation incorporating a three sections distribution of K, *Acta. Meteor. Sinica.*, **46:** 267-275 (in Chinese with English abstract).

Zhao, M. (1983). The theoretical distribution of the wind in the PBL with circular isobars, *Boundary layer Meteor.*, **26:** 209-226.

Zhao, M. (1987a). A numerical model of steady and neutral atmospheric boundary layer over water with varying roughness, *Sci. Atmos. Sinica*, **11:** 247-256 (in Chinese with English abstract).

Zhao, M. (1987b). The wind distribution in the nonlinear atmospheric boundary layer of a circular vortex; *Acta Meteor. Sinica*, **45:** 150-158. (in Chinese with English abstract).

Zhao, M. (1987c). On the parametrization of the vertical velocity at the top of the PBL: *Adv. Atmos. Sci.*, **4:** 234-239.

Zhao, M. (1988a). A numerical experiment of the PBL with geostrophic momentum approximation, *Adv. Atmos. Sci.*, **5:** 47-56.

Zhao, M. (1988b). The numerical experiment on applying geostrophic momentum approximation to the baroclinic and non-neutral PBL, *Adv. Atmos. Sci.*, **5:** 384-397.

Zhao, M. (1988c). The numerical model of baroclinic and non-neutral atmospheric boundary layer over sea, to be published in *Sci. Atmos. Sinica*.